Methodology for determining Pseudorange noise and multipath models for a multi-constellation, multi-frequency GBAS system

G. Rotondo[(1)], P. Thevenon[(1)], C. Milner[(1)], C. Macabiau[(1)], M. Felux[(2)], A. Hornbostel[(2)], M. S. Circiu[(2)]
[(1)]Ecole Nationale de L'Aviation Civile
7 Av. E. Belin CS 54005 Toulouse 31000 France
rotondo@recherche.enac.fr
[(2)] German Aerospace Center (DLR), Institute of Communications and Navigation,
Oberpfaffenhofen, 82234 Wessling, Germany

BIOGRAPHIES

Rotondo Giuseppe is a Ph. D. Student at *Ecole Nationale de l'Aviation Civile*, in the SIGnal processing and NAVigation (SIGNAV) research group of the TELECOM Lab., in Toulouse. He is graduated in Sciences and Technologies of the Navigation from the Naples "Parthenope" University in 2012.

Dr. Paul Thevenon graduated as electronic engineer from Ecole Centrale de Lille in 2004 and obtained in 2007 a research master at ISAE in space telecommunications. In 2010, he obtained a Ph.D. degree in the signal processing laboratory of ENAC in Toulouse, France. From 2010 to 2013, he was employed by CNES, the French space agency, to supervise GNSS research activities and measurement campaigns. Since the July 2013, he is employed by ENAC as Assistant Professor. His current activities are GNSS signal processing, GNSS integrity monitoring and hybridization of GNSS with other sensors.

Dr. Carl Milner received his Master of Mathematics degree from the University of Warwick in 2004 and PhD from Imperial College London in 2009. He continues to work on satellite navigation applications within civil aviation as an assistant professor at ENAC

Dr. Christophe Macabiau graduated as an electronics engineer in 1992 from the ENAC in Toulouse, France. Since 1994, he has been working on the application of satellite navigation techniques to civil aviation. He received his Ph.D in 1997 and has been in charge of the signal processing lab of ENAC since 2000. He is now the head of the Telecom Lab at ENAC.

Dr. Michael Felux obtained a diploma in Technical Mathematics from TU München in 2009. He joined the German Aerospace Center (DLR) the same year and has been working mainly on GBAS since then. Currently, he is a Ph.D. candidate at TU München, Chair of Flight System Dynamics.

Dr. Achim Hornbostel holds a diploma degree in electrical engineering and a Ph.D. from the University of Hannover, Germany. He joined the German Aerospace Centre (DLR) in 1989 and is currently head of a working group on algorithms and user terminals at the Institute of Communications and Navigation. His main activities are presently in interference mitigation, hardware simulation and receiver development. He is member of ION, EUROCAE WG62 'Galileo' and VDE/ITG section 7.5 'Wave Propagation'.

Mihaela Simona Circiu is member of the Integrity Group of the Institute of Communications and Navigation at German Aerospace Center. Her research focuses on multi-frequency multi-constellation ground based augmentation system. She graduated as Computer Engineer at Technical University of Iasi, Romania. In 2012, she obtained a 2nd level Specialized Master in Navigation and Related Applications from Politecnico di Torino.

ABSTRACT

The Ground Based Augmentation System (GBAS) is being studied as a potential means to provide Category II/III precision approach operations. The current technology, the Instrumental Landing System (ILS) is expensive to maintain and suffers from multipath effects which inhibit capacity in all-weather conditions. The GBAS Approach Service Types (GASTs) have been defined to apply to the various levels of vertically guided approach for which up to GAST C relating to Category I precision approach have been standardized. GAST D is under development to support Category II/III precision approaches using the L1 C/A signal of the GPS constellation. A GAST F concept is being developed within the SESAR framework on the basis of a multi-constellation (GPS and GALILEO) multi-frequency environment (L1/L5 and E1/E5a). In order to assess which processing models are to be selected for the GAST F solution, the error models for the new signals must be developed taking into account the impact of the antenna and receiver. This paper presents the analysis of the noise and multipath characterisation using real measurements taken at an experimental ground station.

INTRODUCTION

The ILS is used for guiding aircraft on final approach during precision approach operations at almost all the major airports worldwide. The ILS whilst not expensive to

install requires frequent and expensive maintenance. Furthermore, the system can only support a straight-in approach trajectory for a single runway end, such that multiple installations for one airport are required to support multiple runways [1]. Known issues also include multipath caused by uneven ground surface or other aircrafts on the airport surface which limit the capacity by restricting separation minima. Using the Global Navigation Satellite Systems (GNSS) with the GBAS could provide the safe and reliable guidance required with greatly improved flexibility in the definition of approach tracks. Moreover, GBAS could be a more cost effective solution since only one ground subsystem installation could be used to support multiple runway approaches at a single or potentially multiple aerodromes. The GBAS enhances the core constellation by providing differential corrections and integrity monitoring. Different types of services were developed classified with the acronym GBAS Approach Service Type (GAST), with GAST C supporting the Category (CAT) I precision approach type using Single Frequency (SF) and Single Constellation (SC) position solution. GAST D is designated for the Category II/III precision approach operations utilizing the L1 C/A signal of the Global Positioning System. With the advent of GAST D, a secondary shorter smoothing filter time constant of 30s has been introduced to limit the maximum residual differential ionospheric error, whilst GAST C is based on a 100s time constant [1]. Despite this, the primary threat to GBAS users remains the gross ionospheric differential error induced by strong gradients. GBAS like all differential navigation systems relies on strong spatial correlation of errors such as this ionospheric delay between the ground reference stations and aircraft, such that they may be mitigated through the broadcast of corrections. However, extreme ionosphere storms, causing large ionosphere differential errors must be protected against and monitoring for such threats inevitably impacts on continuity and availability, potentially resulting in a degradation of service. One means to overcome this problem is to use the signals on Multiple Frequencies (MF) to form combinations which partially or totally remove the delays caused by the ionosphere [2] [3]. Furthermore, the additional satellites available in the Multiple-Constellation (MC) environment will significantly improve performance by adding geometric redundancy. Dual frequency techniques have been investigated in previous work [4] [5], leading to two smoothing algorithms, Divergence Free (D-free) and Ionosphere Free (I-free) smoothing. The differences between the two algorithms relate to the level of mitigation of the ionospheric delay and the resulting noise inflation of the final observables. The I-free technique removes the ionosphere delay in its entirety but at the cost of increased noise on the observable used for positioning. This is achieved through combining both the code and phase measurements on two frequencies. The D-free technique removes only the part of the ionospheric delay relating to the transient temporal divergence, but no increase in the standard deviation of the noise and multipath over the single frequency smoothing output occurs [4] [5].

These techniques can thus be used to mitigate the ionosphere and provide Cat II/III services when the GAST D service would be unavailable (under ionospheric gradient conditions or under poor geometry conditions). The SESAR 15.3.7 project is developing the GAST F concept through the investigation of these processing methodologies amongst others. In order to assess accurately the performance which may be achieved, the error model for the GALILEO E1 signal, the Galileo E5a signal and the GPS L5 signals must be determined. It is important to determine this firstly at the raw pseudorange level before addressing the impact of smoothing. Furthermore, different smoothing time constants and correction update rates are being considered within the SESAR framework which will require newly characterized models than those presented within the MOPS and SARPs [6] [7]. In addition, new GAST F constraints regarding the antenna environment for the ground installation and on the tracking configuration on the receiver may be defined which would modify the impact of noise and multipath on the measurement.

CURRENT ERROR MODEL

The error model of a GBAS is composed by different errors contributing to the total error model. *The non-aircraft contribution of the residual error* is given in [6] and [8] by the formula:

$$RMS_{pr_{ground}}(\theta_i) \leq \sqrt{\frac{1}{M}\left(a_0 + a_1 e^{\left(-\frac{\theta_i}{\theta_0}\right)}\right)^2 + (a_2)^2} \quad (1)$$

Where:

- M is the number of the receivers in the ground subsystem.
- $\theta_i$is the elevation angle for the i^{th} ranging source.
- The values of a_0, a_1, a_2 and θ_0 are given in Table 1

The main contribution to this type of error is given by noise and multipath at the ground station, other sources of error are due to residual atmospheric error due to the physical separation between the ground station and the aircraft.

Table 1 – Non-Aircraft Elements Accuracy Requirement [6].

GAD	θ_i (degrees)	a_0	a_1	a_2	θ_0 (degrees)
A	>5	0.5	1.65	0.08	14.3
B	>5	0.16	1.07	0.08	15.5
C	>35	0.15	0.84	0.04	15.5
	<35	0.24	0		//

NOISE AND MULTIPATH EVALUATION

The development of a new GBAS service, GAST F, requires the knowledge of the error models for each signal used over the two constellations. The model proposed for until now is adapted only for the GPS L1 signal and considers a smoothing filter time constant of 100 seconds. In GAST F new possible processing options should be used

and consequentially different smoothing time constant, the evaluation of the errors before the smoothing filter in this case can provide precious information to the user.
The evaluation of the multipath plus noise error on L1 has been done using following the formula of the Code-Carrier (CMC) with Divergence-Free combination of the phase measurement [4]. This particular combination of code and dual frequency phase measurement is composed mainly of the noise and multipath error on the code measurement. The equation of the CMC is:

$$CMC_{L1} = \rho_1 - \phi_1 + \frac{2}{\alpha}(\phi_1 - \phi_2) \quad (2)$$

Where:

- ρ_1 is the code measurement on L1;
- ϕ_1 and ϕ_2 are the phase measurement on L1 and L2
- $\alpha = 1 - \frac{f_1^2}{f_2^2}$, f_1 and f_2 are the frequencies of the signals on L1 and L2.

Considering the model of the code and phase measurement as:

$$\rho_1 = r + c(dt^{sv} + dt^{rec}) + T + I_1 + \varepsilon_{\rho 1} \quad (3)$$
$$\phi_1 = r + c(dt^{sv} + dt^{rec}) + T - I_1 + N_1 + \varepsilon_{\phi 1} \quad (4)$$
$$\phi_2 = r + c(dt^{sv} + dt^{rec}) + T - I_2 + N_2 + \varepsilon_{\phi 2} \quad (5)$$

Where:

- r is the true range;
- $dt^{sv/rec}$ are the satellite and receiver clock errors;
- T is the troposheric delay;
- I_1 and I_2 are the ionospheric delay related to the frequency;
- N_1 and N_2 are the phase ambiguities related to each frequency;
- ε is the noise and multipath error on the code or on the phase measurement, according to the frequency.

Replacing the eq. (3), (4) and (5) in eq. (2) and removing all the terms that are common in the three models, the remaining terms are:

$$CMC_{\rho 1} = \left(I_1 + \varepsilon_{\rho 1}\right) - \left(-I_1 + N_1 + \varepsilon_{\phi 1} - \frac{2}{\alpha}\left(-(I_1 - I_2) + (N_1 - N_2) + \left(\varepsilon_{\phi 1} - \varepsilon_{\phi 2}\right)\right)\right) \quad (6)$$

Considering the relation between the ionospheric delay and the frequencies used:

$$I_1 = \frac{I}{f_1^2}; \quad I_2 = \frac{I}{f_2^2} \quad (7)$$

It is possible to compute the following relation:

$$I_1 - I_2 = \left(1 - \frac{f_1^2}{f_2^2}\right) I_1 = \alpha\, I_1 \quad (8)$$

It is possible to replace it in eq. (6) and simplify the common terms in order to obtain:

$$CMC_{\rho 1} = \left(I_1 + \varepsilon_{\rho 1}\right) - \left(I_1 + N_{12} + \varepsilon_{\phi 12}\right) = \varepsilon_{\rho 1} - \left(N_{12} + \varepsilon_{\phi 12}\right) \quad (9)$$

Where:

- $N_{12} = N_1 - \frac{2}{\alpha}(N_1 - N_2)$
- $\varepsilon_{\phi 12} = \varepsilon_{\phi 1} - \frac{2}{\alpha}\left(\varepsilon_{\phi 1} - \varepsilon_{\phi 2}\right)$

In eq. (9) the first term $\varepsilon_{\rho 1}$represents the noise and multipath affecting the code measurement, this error is assumed to be zero mean over long period. The second term is the phase ambiguity combination, it is a constant values and it is easily removable considering that the noise and multipath are zero mean over long period. The last term is a combination of noise and multipath on the phase measurement, as for the noise and multipath on code measurement this error is assumed to be zero mean over long period; this error can be considered as negligible if compared with the same error on the code measurement.
In case of SF data is not available to compute the CMC as in eq. (2), one possible combination is:

$$CMC_{\rho 1} = \rho_1 - \phi_1 = \varepsilon_\rho + \varepsilon_\phi + N_1 + 2I_1 \quad (10)$$

It is possible to see that now the CMC as computed in eq. (10) is affected by the ionospheric delay multiplied by 2. To remove this term from the CMC, it can be computed using the DF measurements from a nearby station; considering the models of the phase measurement and removing the common terms:

$$\phi_1 - \phi_2 = -(I_1 - I_2) + \left(\varepsilon_{\phi 1} - \varepsilon_{\phi 2}\right) \quad (11)$$

Knowing the relation of the ionospheric delay on different frequencies as given in eq. (7), it is possible to replace these relations in eq. (11) and it is possible to find the following relationship:

$$\phi_1 - \phi_2 = -I\left(\frac{(f_2^2 - f_1^2)}{f_1^2 f_2^2}\right) + \left(\varepsilon_{\phi 1} - \varepsilon_{\phi 2}\right) \quad (12)$$

Where I is the ionospheric delay not related to any frequency.
Just multiplying all the terms by $f_2^2/(f_1^2 - f_2^2)$, it is possible to obtain:

$$\frac{f_2^2}{f_1^2 - f_2^2}(\phi_1 - \phi_2) = \frac{I}{f_1^2} + \frac{f_2^2}{f_1^2 - f_2^2}\left(\varepsilon_{\phi 1} - \varepsilon_{\phi 2}\right) \quad (13)$$

In eq. (13) the first term, $\frac{I}{f_1^2}$ is the ionospheric delay on the same frequency as the code measurement; the last one is the difference of noise and multipath on the phase measurement multiplied by a term related to the two used frequency; this second term is negligible if compared to the ionospheric delay.

It is therefore possible to evaluate the term I_1 from a dual frequency phase combination of a nearby station, and to remove the influence of the ionosphere in eq. (10).

When applying directly one of the two formula for the CMC computation, it is possible to see some large errors affecting it, which is not representing the multipath or the noise error, but is in fact due to phase ambiguity in Eq. (2). This effect is visible in Figure 1.

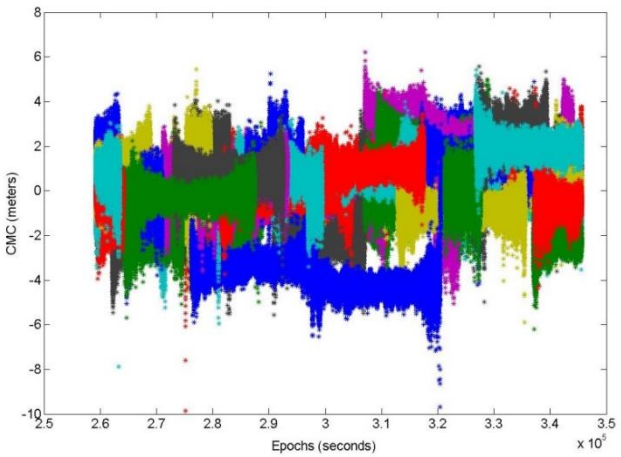

Figure 1 – Multipath and Noise Evaluation on L1

In order to have the correct evaluation of the multipath plus noise impact on the L1 and L5 signals, the following work has been done:

- Identify groups of data corresponding to a continuous tracking of the signal.
- Search inside each group of data for possible cycle slip comparing the predicted phase measurement, eq. (14), and the real one [10]:

$$\widehat{\Phi}_k = \Phi_{k-1} + \frac{\dot{\Phi}_k + \dot{\Phi}_{k-1}}{2}\,\Delta t \qquad (14)$$

Where

- $\widehat{\Phi}$ is the predicted phase measurement
- Φ is the real phase measurement.
- $\dot{\Phi}$ is the Doppler measurement
- k is the epoch index
- Δt is the interval between the k^{th} measurement and the previous one.

If the absolute difference between the real phase measurement and the predicted phase is bigger than 1 cycle or 1 wavelength, a cycle slip is detected.

If no Doppler measurement are present in the data another methodology must be used. The computation of the double-differences on the phase measurement can be used to detect cycle slip [11]:

$$d_i = \phi_{I+1} - \phi_i$$
$$dd_i = d_i - \frac{d_{i+1} + d_{i-1}}{2} \qquad (15)$$

The cycle slip is detected by comparing the value of the real and predicted phase measurement, the threshold has been set at 1 cycle. For the case with the double-differences, the threshold is 0.5.

From each CMC series, according to the group of data, the mean value of the CMC is removed in order to compensate for the possible phase ambiguity over the measurement. It is important to note that because noise and multipath are assumed to be zero mean over long period, the slices of CMC with less than 3000 samples are not taken into account. In Figure 2 it is possible to see that the cycle slips and the phase ambiguity are removed from the CMC.

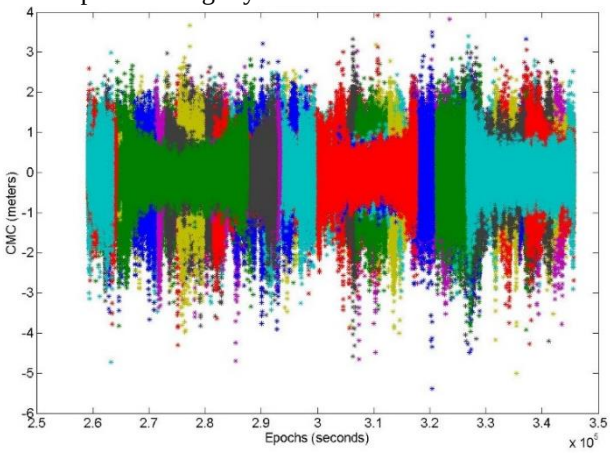

Figure 2 - Multipath & Noise on L1 Corrected for the Phase Ambiguity

Once that the CMC has been computed, the modelling of the error for each satellite and for a 1° elevation bin is done. An auto-regressive (AR) model is used because it is a more realistic representation of the noise plus multipath signal, in fact it takes into account the correlation time of the data. The representation of the signal just using sigma as representation of the standard deviation and considering it as white noise is a too optimistic representation for processing purposes. A generic AR model is represented by the following formula [12]:

$$x(n) = -\sum_{k=1}^{p} a_k x(n-k) + b(n) \qquad (16)$$

Where

- x is the signal at different lags.
- a_k are the coefficients according to order model.
- $b(n)$ is a Gaussian noise, named the driving noise.

The goal of the modelling process is to estimate the a parameters, according to the model order, and the variance or the standard deviation of the driving noise for each elevation bin. Different Matlab functions are used in order to compute the a parameters and the variance of the driving noise, then a comparison between the function has been done on order to check possible differences. They are all computing the same parameters, but using different methods.

LPC (data, order). This function find the coefficients of N-order forward linear prediction and the variance of the driving noise.

ARCOV (data,order) Estimate AR model parameters using covariance method and the variance of the driving noise.

ARYULE (data,order) Estimate autoregressive (AR) all-pole model using Yule-Walker [13] method and variance of the driving noise.

ARMCOV (data,order) Estimate AR model parameters using modified covariance method and compute the variance of the driving noise.
ARBURG (data,order) Estimate AR model parameters using Burg [14] method and compute the variance of the driving noise.
These different methods all estimate the parameters of an AR model, but use different computation techniques. The following investigation aims at determining if one of these methods is more appropriate to the targeted kind of data.

RESULTS

The methodology explained in the previous chapter has been applied on two series of measurement:

1. Data collected at Braunschweig airport by DLR the 9th July 2014. The first observation available is at 00h 00' 00" and the last observation is at 23h 59' 59", the interval between the observations is 0.5 seconds. The antenna model is a Leica AR-25 choke ring antenna the stations are located at the positions given in Table 2.
2. Data Collected at Malaga airport GBAS Station (courtesy of ENAIRE) the 30th March 2014. The first observation available is at 00h 00' 14" and the last one is the day after at 00h 00' 14". The measurement are recorded at 2 Hz only for the GPS L1 C/A signal, data coming from the near monitoring station have been also used to compute the ionospheric delay. The antenna, for the GBAS data, is a Multipath Limiting Antenna (MLA).

Table 2 – Reference Receiver Locations

Indicator	Latitude[°]	Longitude[°]	Receiver Type
BR01	52.321444 N	10.543339 E	Javad Delta
BR02	52.322324 N	10.554618 E	Javad Delta
BR03	52.317001 N	10.567265 E	Javad Delta
BR04	52.321269 N	10.564586 E	Javad Delta

DLR data collection

The first step is the choice of the order model, it derives from the analysis of three different criteria that provide an estimation of the prediction error power [15] and are commonly used to determine the order of an auto-regressive model. The criteria are:

- The Final Prediction Error (FPE)
- The Akaike Information Criterion (AIC)
- The Criterion Autoregressive Transfer (CAT).

$$FPE(k) = \frac{N+k}{N-k}\, C \qquad (17)$$

$$AIC(k) = N\ \ln(C) + k\ \ln(N) \qquad (18)$$

$$CAT(k) = \frac{N}{N-k}\, C \qquad (19)$$

Where

- k is the model order
- C is the power of the prediction error
- N is the number of signal samples

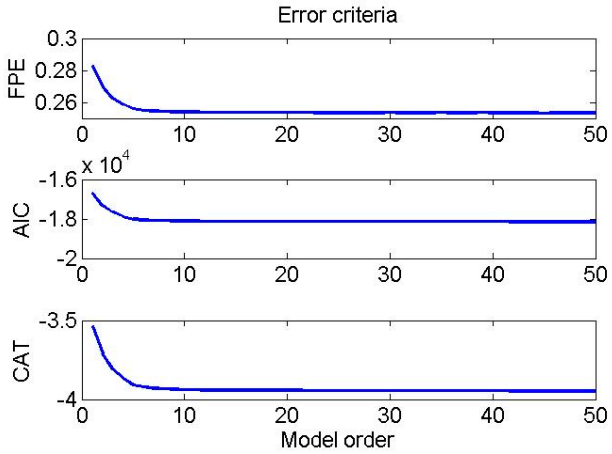

Figure 3 – Error Criteria for Satellite PRN 5

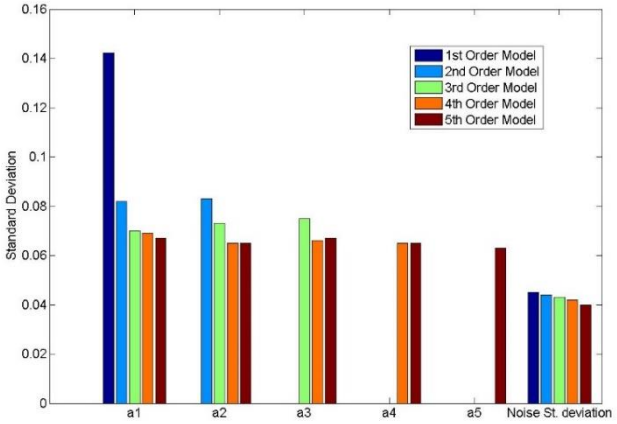

Figure 4 – Coefficients and Driving Noise Standard Deviation for Different Model order

Figure 3 shows that the practical minimum order is around 5, however analyzing also the errors magnitude for the lower model order has been found that the difference of the error criteria between the second and the fifth order model is small (approximately between 6-7 % for each criteria). Therefore, a 2nd order model seems reasonably close to represent the real signal, and has the benefit to keep the model simpler than a higher order model.
In Figure 4, the comparison of the coefficients standard deviation confirms the choice of the model. The standard deviation of the a1 coefficients for the 1st order model is larger than the other model orders, and from the second order, the standard deviation starts to be almost similar. The values of the a2 standard deviation are similar for all the order model analyzed. The standard deviation of the

driving noise is similar for all the model orders analyzed. From the previous analysis the second order model has been selected to model the noise and multipath, the equation that model the noise and multipath is:

$$x(n) = -a_1 * x(n-1) - a_2 * x(n-2) + b(n) \quad (20)$$

In the next figures the values of the a coefficients and the standard deviation of the driving noise process will be show, the red lines represent the proposed coefficients and the proposed model for the noise standard deviation.

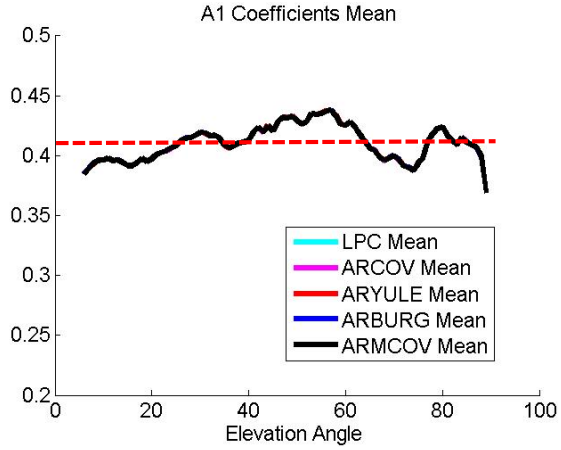

Figure 5 - A1 Coefficients: Mean Values and Related Standard Deviation

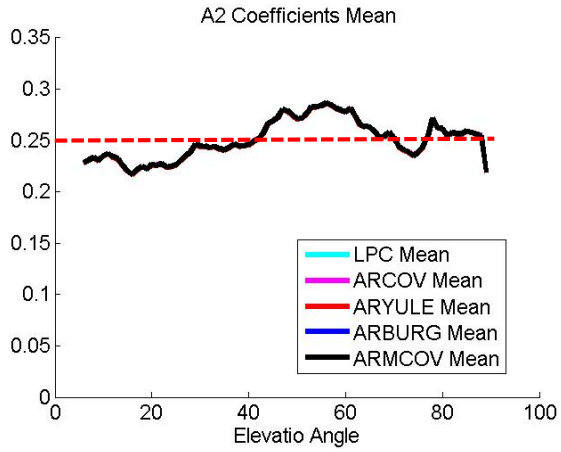

Figure 6 - A2 Coefficients: Mean Values and Related Standard Deviation

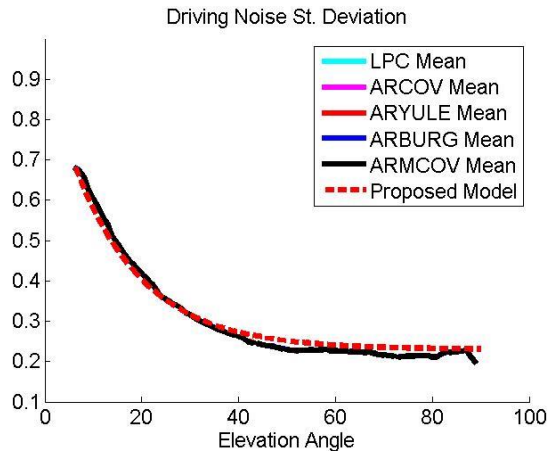

Figure 7 – Noise Mean Values and Proposed model Each Elevation Bin

From the analysis of the previous figures, it is possible to assess that for the analyzed data there are no differences in the coefficients computed with the different Matlab functions and even the standard deviation is similar for all of them; for this reason in the next figures just the ARMCOV function will be considered. The a_1 coefficient model proposed is 0.41, instead the value of a_2 coefficient model is 0.25. The standard deviation of the driving process noise follows an elevation dependent exponential curves, the model proposed for it is:

$$\sigma_{dr\_noise} = 0{,}7 * exp^{-\frac{El}{14{,}3}} + 0{,}23 \quad (21)$$

And it is represented by the red dashed line.

In order to be sure that the computed coefficients and variance of the driving noise are consistent, the real signal and the one generated by the use of the model parameters are compared in Figure 8, and an analysis if the autocorrelation function is shown in Figure 9. These plots show that the coefficients of the model reflects the properties of the real signal.

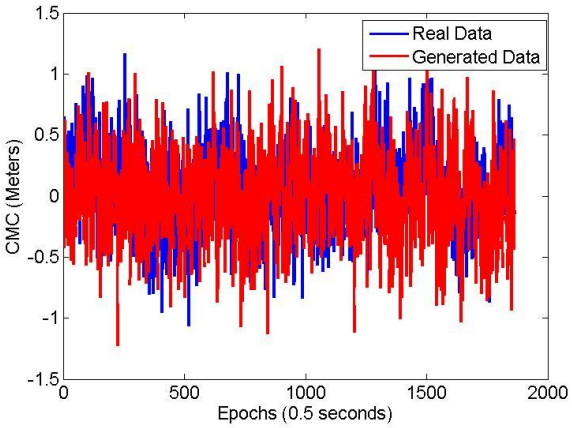

Figure 8 – Real CMC and Generated CMC for Satellite PRN 2 and 30° Elevation Bin

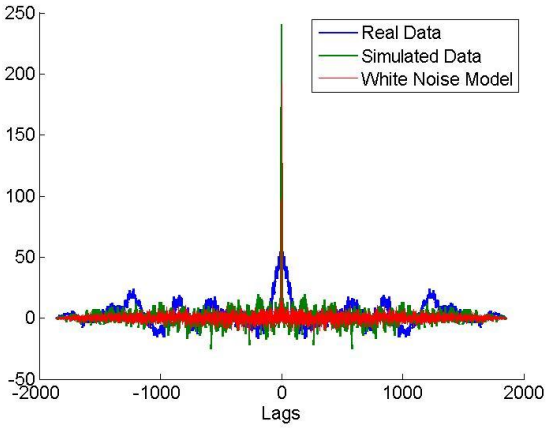

Figure 9 – Autocorrelation Function for Satellite PRN 2 and 30° Elevation Bin

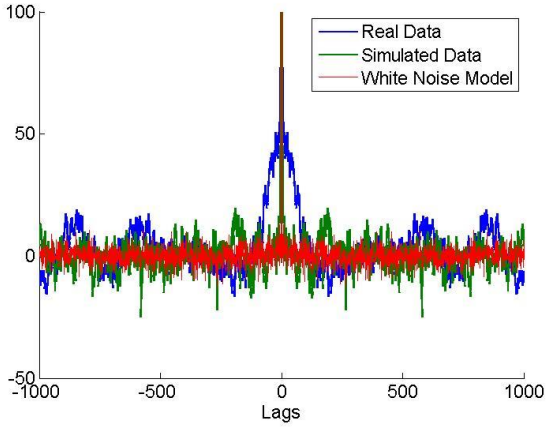

Figure 10 – Autocorrelation Function for Satellite PRN 2 and 30° Elevation Bin (zoom from – 1000 to 1000)

Malaga GBAS station data collection

As for the previous set of data, the first step is the choice of the model order. Using the same methodology explained before the analysis of the FPE, AIC and CAT has been done followed by the analysis of the coefficient's standard deviation.

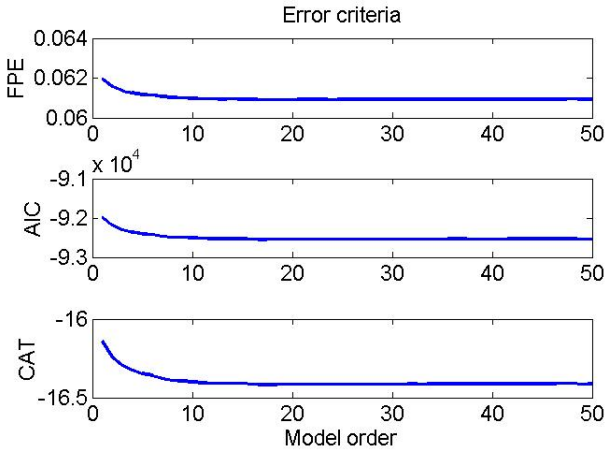

Figure 11 – Error Criteria for Satellite PRN 3

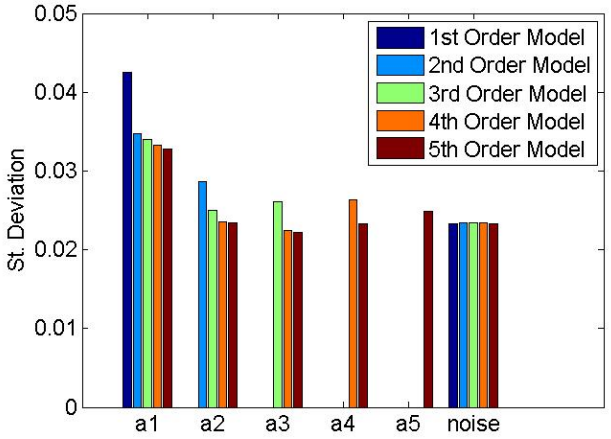

Figure 12 – Coefficients and Driving Noise Standard Deviation for Different Model order

The analysis of Figure 11 shows that the practical model order is at 10, but analyzing also the lower model order error magnitude, it is possible to see that the magnitude of the three criteria for the first model order is at most 3% bigger than the one provided by model order 10.

The choice of the 1st model order seems to be appropriate in order to have a reasonably accurate model but not too complex. The analysis of Figure 12 shows that the standard deviation of the a_1 coefficients is really similar for all the model order and also the driving noise standard deviation has almost the same values for all the order models. Thanks to these two analysis is possible to select 1 as model order. The equation of the autoregressive model, for this set of data, is:

$$x(n) = -a_1 * x(n-1) + b(n) \qquad (22)$$

The next plots will show the a_1 coefficients mean and the driving noise standard deviation computed for all the elevation angle between 10 and 90.

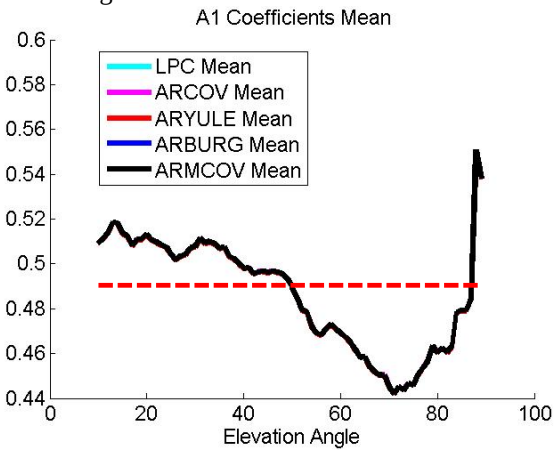

Figure 13 – A1 Coefficients: Mean Values and Related Standard Deviation

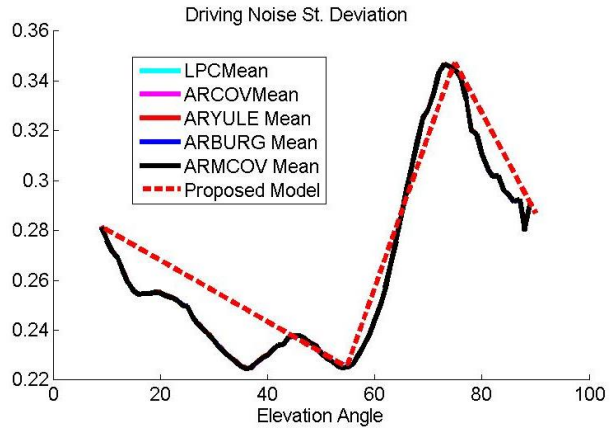

Figure 14 - Noise Mean Values and Proposed model Each Elevation Bin

From the analysis of the previous figures, it is possible to assess that for the analyzed data, there are no differences in the coefficients computed with the different Matlab functions and even the standard deviation is similar for all of them; like for the previous case in the next plot only the ARMCOV function will be used. The a_1 coefficient model proposed is 0.49, the standard deviation of the driving process noise has a constant value until 60° elevation angle and after follows an elevation dependent curves, the model proposed for it is:

- $-0.00123 * El + 0.2629$ between 10° and 55° elevation angle
- 0.0061*El-0.109*El.-0.3 for elevation angle between 55° and 75°
- -0.004*El+0.6471 for elevation angle bigger than 75°

As for the previous data analysis, the next two plots will show the comparison between a slice of the real CMC and the generated one using the AR model and the related autocorrelation function.

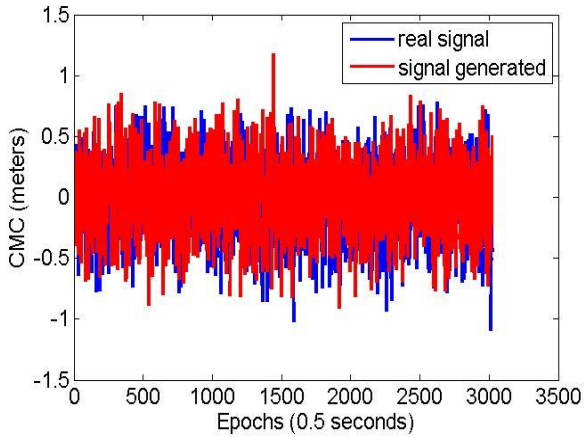

Figure 15 – Real CMC and Generated CMC for Satellite PRN 18 and 30° Elevation Bin

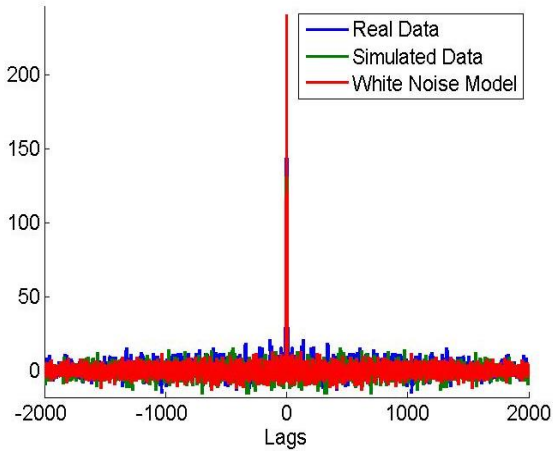

Figure 16 – Autocorrelation Function for Satellite PRN 18 and 30° Elevation Bin

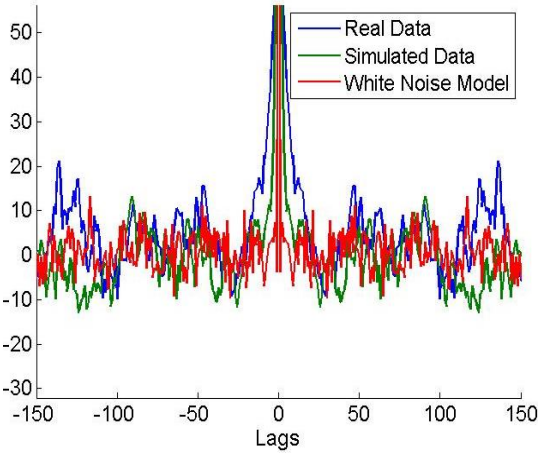

Figure 17 – Autocorrelation Function for Satellite PRN 18 and 30° Elevation Bin (zoom from – 150 to 150)

20th Order model analysis

The aim of this part is to show the results obtained using the 20th order model to generate the CMC. In order to have a better comparison between orders model the same slices of signal that have been used in the previous chapter will be used.

The first plots show the results obtained for the DLR data collection.

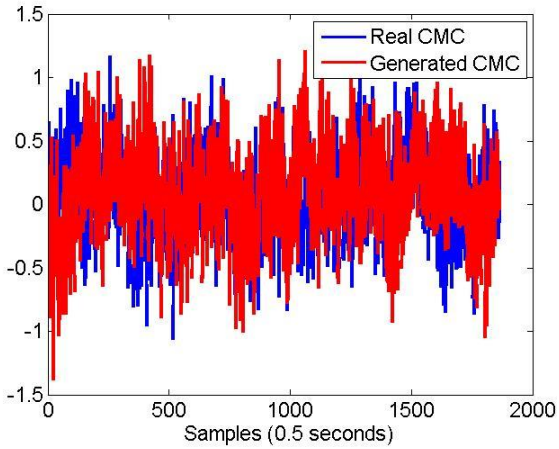

Figure 18 – Real CMC and Generated CMC for Satellite PRN 2 and 30° Elevation Bin with a 20th order model

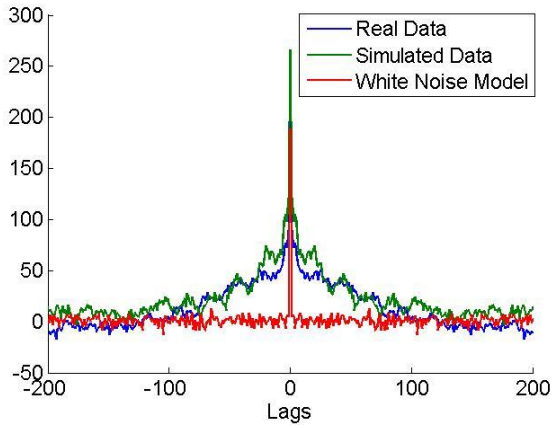

Figure 19 – Autocorrelation Function for Satellite PRN 2 and 30° Elevation Bin (zoom from – 200 to 200) with a 20th order model

As it is possible to see, using the 20th order model the signals have the same statistical property and the autocorrelation functions have the same shape.
In the next plot the results obtained by applying order model 20 to the Malaga airport data collection will be shown.

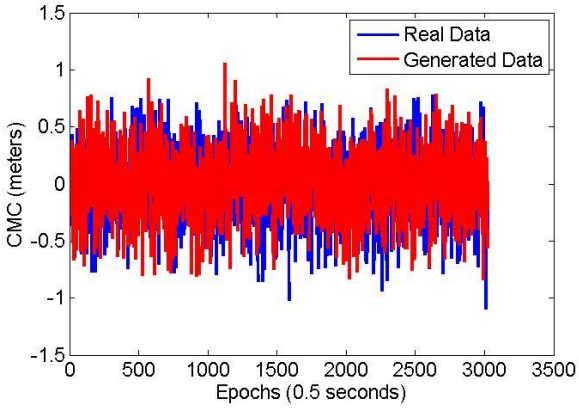

Figure 20 – Real CMC and Generated CMC for Satellite PRN 18 and 30° Elevation Bin with a 20th order model

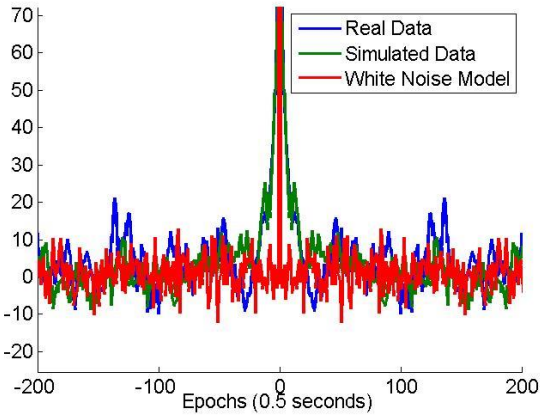

Figure 21 Figure 22 – Autocorrelation Function for Satellite PRN 18 and 30° Elevation Bin (zoom from -200 to 200) with a 20th order model

From the previous two figures it is possible to see that the use of order model 20 permit to have an autocorrelation function, of the generated data, similar to the one of the real data.

CONCLUSION

We have presented a proposal for the estimation of noise and multipath using a D-Free combination. In order to remove possible phase ambiguity and cycle slip on the phase a phase based cycle slip detector has been implemented, finally the CMC was modelled using an autoregressive method. The application of this methodology to two different data collections using only single ground receiver, has provided good results; however it is important to note that the results provided for the DLR data collection are not representative of a certificated GBAS ground station because they are not conform with the siting antenna and receiver constraints. One advantage of this method is that it provides more information about the noise and multipath temporal correlation than just describing the time series by its total standard deviation.

FUTURE WORKS

The next steps of this work consists in the application of the methodology to a large set of data and in particular to GPS L1 and L5 and GALILEO E1 and E5a, which will be the signal of interest of a GAST F GBAS system. The second step will be the analysis of the same signal applying the I-Free combination and, finally, the analysis of the two combinations after the smoothing filter using different smoothing time constants in order to verify their impact on the noise and multipath pseudorange error. The correct model of noise and multipath standard deviation vs. elevation will then be used for other measurement processing in the GAST F GBAS system, such as the computation of the Protection Levels.

ACKNOWLEDGMENTS

The authors would like to thank DLR and INDRA/ENAIRE for provision of data and for supporting the work.

REFERENCES

[1] Dautermann, T., Felux, M., Grosch, A., (2011). Approach service type D evaluation of the DLR GBAS testbed. *GPS Solutions*, Springer-Verlag 2011.

[2] Circiu, M-S., Felux, M., Remi, P., Yi, L., Belabbas, B., Pullen, S., "Evaluation of Dual Frequency GBAS Performance Using Flight Data," *Proceedings of the 2014 International Technical Meeting of The Institute of Navigation*, San Diego, California, January 2014, pp. 645-656.

[3] H. Konno "Design of an aircraft landing system using dual-frequency GNSS," *Ph.D. thesis, December 2007*

[4] Konno, Hiroyuki, "Dual-Frequency Smoothing for CAT III LAAS: Performance Assessment Considering Ionosphere Anomalies," *Proceedings of the 20th International Technical Meeting of the Satellite Division of The Institute of Navigation (ION GNSS 2007)*, Fort Worth, TX, September 2007, pp. 424-437.

[5] Hwang, P. Y., McGraw, G. A., & Bade, J. R. (1999). Enhanced DifferentialGPS Carrier-Smoothed Code Processing Using Dual-Frequency Measurements. *Journal of The Institute of Navigation*, Vol 46 number 2.

[6] RTCA DO245A (2004) Minimum aviation system performance standards for the local area augmentation system (LAAS), Tech Rep, DO245A, RTCA.

[7] ICAO NSP May 2010 WP 59, "Development Baseline SARPs Proposal", presented by Tim Murphy, Montreal, 17-28 May 2010.

[8] ICAO. (2006). International Standards and Recommended Practices, Annex 10 to Convention on International Civil aviation, Volume I, Radio Navigation Aids, Sixth Edition.

[9] Booth, J., Murphy, T., Clark, B., Liu, F. (2000). Validation of the Airframe Multipath Error Allocation for Local Area Differential GPS. Proceedings of the IAIN World Congress in association with the U.S. ION ANNUAL MEETING, 26-28 June 2000, San Diego, CA

[10] Wang, C. (2003). Development of a Low-Cost GPS-based Attitude Determination System. Ph.D. Thesis, Univursity of Calgary, June 2003

[11] NLR-TR-2003-019, H. Kannemans, Cycle slip detection for static and moving receivers, January 2003

[12] Jackson, L.B., Digital Filters and Signal Processing, Second Edition, Kluwer Academic Publishers, 1989.

[13] Hayes, Monson H. *Statistical Digital Signal Processing and Modeling*. New York: John Wiley & Sons, 1996.

[14] Kay, Steven M. *Modern Spectral Estimation: Theory and Application*. Englewood Cliffs, NJ: Prentice Hall, 1988.

[15] Ljung, L. *System Identification: Theory for the User*, Upper Saddle River, NJ, Prentice-Hal PTR, 1999.